مؤتمر الأزهر الهندسي الدولي التاسع

AL-AZHAR ENGINEERING
NINTH INTERNATIONAL CONFERENCE
April 12 - 14, 2007

Code : M 18

INTERACTION OF SURFACE RADIATION WITH NATURAL CONVECTION AIR COOLING OF DISCRETE HEATERS IN A VERTICAL RECTANGULAR ENCLOSURE

R.Y. Sakr[1] and T.A. Ahmed[2]
[1] Mech. Eng. Dept., Shoubra Faculty of Engineering, Benha University, Egypt
[2] Mech. Power Eng. Dept., Faculty of Engineering , Cairo University, Egypt

ABSTRACT
This paper presents a numerical study that concerning the effect of surface radiation on natural convection cooling of four discrete isoflux heaters flush-mounted on a vertical wall of an air filled rectangular enclosure. The opposite side is isothermally cooled while the top and bottom sides as well as the spacing between the heaters are kept adiabatic. Two-dimensional mathematical model was developed based on solving the partial differential equations for the conservation of mass, momentum, and energy. A laminar flow is to be considered in the present model. Galerkin finite element method was utilized for the model formulation.

A numerical simulation is carried out to examine the parametric effects of enclosure aspect ratio, Rayleigh number, heater emissivity, adiabatic and cold surfaces emissivities, and the radiation parameter on the role played by the surface radiation in heat dissipation from the discrete heaters in the enclosure. The computed model results were verified through the comparison with those experimental results available in the literature and good agreement between them were noticed.
Several correlation equations in terms of aspect ratio, Rayleigh number, heater surface emissivity and the radiation parameter for the average Nusselt number for heaters, its radiative and convective components as well as the maximum surface temperature at the discrete heaters are obtained.

KEYWORDS : Natural Convection; Surface Radiation

1. INTRODUCTION
In the recent years, much attention is being paid to many practical applications involving heat transfer in vertical enclosures. Electronic equipment cooling, efficient building heating and design of solar collectors are some examples of these applications. Natural

convection cooling techniques have distinct advantages because of their low cost, easy maintenance and the absence of electromagnetic interface and operating noise. Although in most cases the flow is three dimensional, two-dimensional results are satisfactory, especially when considering the large reduction in computational effort. Comprehensive reviews of natural convection electronic cooling are available [1,2]. Under certain circumstances, such as operation in dusty or hazardous environment, electronic components are packaged within sealed enclosures. The components may be mounted to one vertical wall of the enclosure, while the other walls are cooled. This geometry is one of the fundamental configurations encountered in thermal management of electronic equipment and has received extensive attention since the pioneering study of Chu et al. [3] as indicated by the references cited in the recent works [4-6]. In most cases, there is an interaction of surface radiation and natural convection in many analyses. This interaction is omitted due to low emissivities, then radiation contribution has been taken care of by adding a correction using simple formulae like that between infinite parallel plates facing each other, Hoogendoorn [7].

NOMENCLATURE

A	element area	W	enclosure width, m
AR	aspect ratio H/W	x, y	Cartesian coordinates
dn	distance between two adjacent nodes in the normal direction to the wall boundary	X, Y	dimensionless Cartesian coordinates x/W, y/W
E	total number of elements		
F_{ij}	shape factor between surfaces i, j	***Greek symbols***	
{F}	load vector, Eq. (16).	α	Thermal diffusivity of the fluid, m^2/s
g	gravity vector	β	thermal expansion coefficient**,** 1/K
G	bounded domain	Γ	domain boundary
h	heat transfer coefficient, W/m^2K	θ	dimensionless temperature
H	enclosure height	ν	Viscosity**,** kg/m.s
J	dimensionless radiosity	ρ	Density**,** kg/m^3
k	thermal conductivity, W/mK	ψ	stream function**,** m^2/s
[K]	stiffness matrix	Ψ	dimensionless stream function**,** ψ/α
l	heater length, m	ε	surface emissivity
L	dimensionless heater length, *l*/W	σ	Stefan-Boltzmann constant, $5.667x10^{-8}$ W/m^2K^4
$N_{1,2,3}$	interpolation functions		
NNS	total number of radiation surfaces	ω	vorticity, 1/s
N_R	radiation parameter, $\sigma T_c^4 / q_h$	Ω	dimensionless vorticity, $\omega W^2/\alpha$
Nu_c	convection Nusselt number	ΔN	dimensionless distance between two adjacent nodes in the normal direction to the wall boundary.
Nu_R	radiation Nusselt number		
Nu	total Nusselt number		
Pr	Prandtl number, ν/α		
q^*	heat flux, W/m^2	***Superscripts***	
q_h	heat flux of heater, W/m^2	e	element level
q	dimensionless heat flux,	T	Transpose
Ra	modified Rayleigh number, $g \beta q_h W^4/(k\nu\alpha)$	R	Radiation
s	spacing between heaters, m		
S	dimensionless spacing between heaters, s/W	***Subscripts***	
T	temperature, K	a	Adiabatic
TR	temperature ratio, T/T_c	c	Cold
u	velocity component in x-direction	h	hot, heater
v	velocity component in y-direction	R	radiation
		w	wall

There are a few studies available in the literature concerning the effect of radiation exchange among surfaces of an enclosure bounding a non-participating fluid. The interaction of surface radiation with transient natural convection in an air-filled rectangular cavity surrounded by one-dimensional conducting walls was analyzed numerically by Larson and Viskanta [8]. Their work was further extended by Kim and Viskanta [9] by considering two-dimensional conduction in the cavity walls.

Balaji and Venkateshan [10] studied the effect of surface radiation on natural convection in a rectangular enclosure. Their model is based on Gosman's finite volume method. A careful review of the literature suggests that the work of Asako and Nakamura [11] is one of the earnest attempts to probe into the effect of surface radiation on natural convection in an enclosure.

For the interaction of surface radiation with natural convection in a discretely heated enclosure, there exists a very little previous work in the literature. Ho and Chang [12] presented basic insights of the role played by surface radiation in cooling of multiple discrete heaters enclosed in a vertical rectangular enclosure. They achieved their analysis numerically by using a finite difference method. In this paper, a parametric study to investigate the interaction of surface radiation with natural convection in a discretely heated enclosure having different aspect ratios using Galerkin finite element method is carried out.

2. MATHEMATICAL FORMULATION

The present problem is illustrated schematically in Fig. (1). Simultaneous heat dissipation by natural convection and surface radiation from four discrete flush-mounted heaters of iso-flux q_h on the left vertical wall of an air filled rectangular enclosure. The enclosure width and height are W and H respectively. The discrete heaters of lengths, *l*, are located uniformly with spacing, s. The right vertical wall of the enclosure is isothermally kept at temperature T_c; and the horizontal walls as well as the left vertical regions between the discrete heaters are assumed adiabatic. The multi-mode heat transfer process within the enclosure is modeled as two-dimensional, steady and laminar natural convection with simultaneous radiation exchange between the end walls of the enclosure. The air is assumed to be radiative non-participating with constant properties and Boussinesq approximation is assumed to be valid. Viscous dissipation and compressibility effects are also neglected.

2.1 Governing Equations

The dimensionless governing equations for the problem can be expressed in terms of temperature, vorticity, and stream function as follows:

$$\frac{\partial \Psi}{\partial Y}\frac{\partial \Theta}{\partial X}-\frac{\partial \Psi}{\partial X}\frac{\partial \Theta}{\partial Y}=\frac{\partial^2 \Theta}{\partial X^2}+\frac{\partial^2 \Theta}{\partial Y^2} \tag{1}$$

$$\frac{\partial \Psi}{\partial Y}\frac{\partial \Omega}{\partial X}-\frac{\partial \Psi}{\partial X}\frac{\partial \Omega}{\partial Y}=Ra\,\mathrm{Pr}\frac{\partial \Theta}{\partial X}+\mathrm{Pr}\left(\frac{\partial^2 \Omega}{\partial X^2}+\frac{\partial^2 \Omega}{\partial Y^2}\right) \tag{2}$$

$$\frac{\partial^2 \Psi}{\partial X^2}+\frac{\partial^2 \Psi}{\partial Y^2}=-\Omega \tag{3}$$

2.2 Boundary Conditions

1- The dimensionless temperature boundary conditions may be written as follows:

$$\text{At}\quad X=0,\ -\frac{\partial \Theta}{\partial X}+q^R=1.0\ \text{(at heaters)},\ -\frac{\partial \Theta}{\partial X}+q^R=0.0\ \text{(elsewhere)} \tag{4a}$$

At X=1, $\Theta = 1.0$ (4b)

At Y=0, 0≤X ≤1.0 $-\frac{\partial \Theta}{\partial X} + q^R = 0.0$ (4c)

At Y=AR, 0≤X≤1.0 $-\frac{\partial \Theta}{\partial X} + q^R = 0.0$ (4d)

Where; the dimensionless local radiative heat flux $q^R=(q^{R*}/q_h)$ can be evaluated by solving the equations for radiative exchange between the end walls of the enclosure. The net radiative flux at any point on the enclosure surface i, can be expressed as:

$$q_i^R = \left(\frac{\varepsilon_i}{1-\varepsilon_i}\right)\left[NR.TR^4 - J_i\right] \quad (5)$$

Where; TR = T/T_c $N_R= \sigma T_c/q_h$

The dimensionless radiosity J_i for the i th surface element can be determined by solving the following equation:

$$J_i = \varepsilon_i + (1-\varepsilon_i)\sum_{j=1}^{NNS=84} F_{ij} J_j \quad (6)$$

The shape factors F_{ij}, between the two surfaces i, j in the above equation can be determined by different formulae according to the relative position between surfaces. In the present study, F_{ij} is calculated by using the crossed string method [13].

2- Stream function boundary conditions

At the solid wall boundaries the values of velocity components u and v are zero; so

$$\frac{\partial \Psi}{\partial Y} = 0.0 \quad (7a)$$

$$\frac{\partial \Psi}{\partial X} = 0.0 \quad (7b)$$

Equations (7a) and (7b) indicate that the magnitude of the stream function over the wall , Ψ_w , is constant. Moreover, Ψ_w is usually assigned a value of zero on the solid boundaries so, $\Psi_w = 0.0$ (8)

3- Vorticity boundary conditions

By using the definition of the vorticity and applying no-slip boundary condition the following equations can be written;

$$\omega = -\frac{d^2\psi}{(dn)^2} \quad (9)$$

Equation (9) can be approximated by using finite difference formulas and then expressed in terms of dimensionless variables as follows:

$$\Omega_w = \frac{2(\Psi_{w+1} - \Psi_w)}{(\Delta N)^2} \quad (10)$$

where;

w refers to the nodal value at the no slip wall.

w+1 refers to the adjacent interior node.
ΔN is the dimensionless distance separating this node pair.

Equations (1), (2) and (3) are solved with the relevant boundary conditions given by Eqs. (4), (8) and (10) to determine the temperature, vorticity and stream function distributions.

2.3 Heat Transfer

The local Nusselt number at the discretely heated surfaces is defined by [14]:

$$Nu_h = \frac{1}{\theta_h} \tag{11}$$

and the average Nusselt number is given by:

$$\overline{Nu} = \frac{1}{H_h} \int Nu_h dL \tag{12}$$

This average Nusselt number is due to the contribution of both natural convection and surface radiation heat transfer modes. So, the average Nusselt number due to radiation and convection can be written as:

$$Nu_R = \left(\frac{q_R}{q} \right) \overline{Nu} \tag{13a}$$

$$Nu_c = \left(\frac{q_c}{q} \right) \overline{Nu} \tag{13b}$$

3. NUMERICAL SOLUTION AND FINITE ELEMENT FORMULATION

The system of equations (1), (2) and (3) forms a set of quasilinear elliptic equations. So, the solutions of the system of equations for Ψ, Ω and Θ will be continuous in the domain G. Hence, the system of equations was solved through an iterative procedure. Initially the stream function is assumed to have a zero value everywhere and Eq. (1) is then solved as a linear equation for Θ. This solution describes the temperature distribution for the pure conduction case. This temperature distribution and the associated stream function field are then substituted into Eq. (2) from which Ω is obtained. Finally the obtained votricity distribution is used in Eq. (3) and an improved value of Ψ is obtained. The cycle of iteration is repeated until the values of Ψ for two consecutive calculations are within 10^{-4}.

The system of equations (1-3) is solved using the Galerkin based finite element method [15, 16]. The objective of the finite element is to reduce the system of governing equations into a discretized set of algebraic equations. The procedure begins with the division of the continuum region G, of interest into a number of simply shaped regions called finite elements.

The Finite Element Formulation

The temperature, vorticity and the stream function in any element (triangle) of the discretized domain as shown in Fig. (1b) can be represented in terms of nodal temperature, vorticity and stream function respectively by the following simple polynomials:

$$\Theta^e = \sum_{m=1}^{3} N_m \Theta_m \tag{14a}$$

$$\Omega^e = \sum_{m=1}^{3} N_m \Omega_m \tag{14b}$$

$$\Psi^e = \sum_{m=1}^{3} N_m \Psi_m \tag{14c}$$

where;

$$N_1 = \frac{1}{2A}\,(a_1 + b_1 X + c_1 Y) \tag{15a}$$

$$N_2 = \frac{1}{2A}\,(a_2 + b_2 X + c_2 Y) \tag{15b}$$

$$N_3 = \frac{1}{2A}\,(a_3 + b_3 X + c_3 Y) \tag{15c}$$

where;

A = area of the triangle 123

$a_1 = X_2Y_3 - X_3Y_2$

$b_1 = Y_2 - Y_3$

$c_1 = X_3 - X_2$

The interpolation functions [N_1, N_2, N_3] in Eqs. (14) are derived from an assumption of linear variation of temperature, vorticity and stream function in the element. The approximate expressions of the system variables are substituted into the governing equations (1)-(3) and the global errors are minimized using the above interpolation functions N_i (i = 1, 2, 3) as weighting functions. The solution of Eqs. (1), (2) and (3) that satisfies the boundary conditions given by Eqs. (4), (8) and (10), can be written after weighted integration over the domain G and the application of Green's theorem, in the equivalent matrix form as:

$$[K_1]\{\Theta\} = \{F_1\} \tag{16a}$$

$$[K_2]\{\Omega\} = \{F_2\} \tag{16b}$$

$$[K_3]\{\Psi\} = \{F_3\} \tag{16c}$$

where,

$[K_1] = [K_I] + [K_{II}]$

$$[K_I] = \sum_{e=1}^{E} \int_{G^e} \left(\frac{\partial [N]^T}{\partial X} \cdot \frac{\partial [N]}{\partial X} + \frac{\partial [N]^T}{\partial Y} \cdot \frac{\partial [N]}{\partial Y} \right) \mathrm{dG}^e$$

$$[K_{II}] = \sum_{e=1}^{E} \int_{G^e} \left(\Psi_X \frac{\partial [N]}{\partial Y} - \Psi_Y \frac{\partial [N]}{\partial X} \right) dG^e$$

$$\{F_1\} = \sum_{e=1}^{E} \int_{\Gamma^e} [N]^T \frac{\partial N}{\partial X} d\Gamma^e + \sum_{e=1}^{E} \int_{\Gamma^e} [N]^T \frac{\partial N}{\partial Y} d\Gamma^e$$

where;

E = total number of elements, G bounded domain, Γ domain boundary,

$$\Psi_X = \frac{\partial \Psi}{\partial X}, \quad \Psi_Y = \frac{\partial \Psi}{\partial Y}$$

Similarly, $[K_2]$, $[K_3]$, $\{F_2\}$and $\{F_3\}$ can be written in the same manner. Equations (16a, 16b, 16c) give three sets of linear equations which have been solved by Gauss

elimination method. The finite element formulation and the resulting linear equations were solved through a computer program written here in FORTRAN code.

4. MODEL VALIDATION

To check the consistency and reliability of the present analysis, the same conditions employed by Ramesh and Venkateshan [17] were used in the predictions. Figure (2) shows the obtained results compared with the experimental data of Ramesh and Venkateshan. Considerable discrepancy is noticed in the case of low cold and hot surface emissivity operating conditions while good agreement is noticed for high emissivity of hot and cold surface emissivity.

5 RESULTS AND DISCUSSIONS

From the foregoing mathematical formulation, the dimensionless parameters that govern the present problem include the modified Rayleigh number Ra, the radiation parameter N_R, and the surface emissivity of the discrete heaters, cold wall and the adiabatic surfaces ε_h, ε_c, ε_a respectively. Furthermore, the problem is solved for different enclosures with different aspect ratios AR. So, numerical calculations have been carried out for rectangular enclosures with the previous parameters having the following ranges: $1 \le AR \le 10$, $10^3 \le Ra \le 5x10^6$, $0.2 \le \varepsilon_h \le 0.8$, and $0.75 \le N_R \le 2.5$. Moreover, the dimensionless heater size *l*/H and spacing s/H on the vertical left side are fixed at 0.033 and 0.173 respectively.

5.1 Flow and Temperature Fields

Figure (3) shows the computed steady-state streamlines and isotherms obtained with the aid of the present numerical scheme for vertical enclosure having four heaters flush mounted on the left side; for AR=5 and $Ra=10^5$. The figure illustrates two cases namely: "without" surface radiation and "with" surface radiation taking radiation parameter $N_R=1.5$, the surface emissivities for heaters, cold and adiabatic surfaces are all equal and having a value of 0.5. The figure indicates that the surface radiation tends to decrease the values of stream functions and temperatures; this means a decrease of the heat transfer by natural convection rate but with an associated enhancement of the overall heat transfer rate. However, these variations are insignificant, which means that the radiation heat transfer at this Rayleigh number is relatively small. But for $Ra=5x10^6$, Fig. (4) shows that, with the coupling of surface radiation, thermal boundary layer along the cold wall tends to degenerate considerably, thereby reducing convective heat transfer rate there. The same behavior can be nearly noticed in Fig. (5) for AR=7, with all other parameters kept unchanged.

5.2 Heat Transfer Results

The effect of Rayleigh number on the heat transfer process that takes place by either radiation or natural convection mode for each discrete heater is illustrated in Fig. (6a-d). The figure shows sharp increase of radiation Nusselt number and slight decrease of convection Nusselt number with the increase of Rayleigh number. Comparing with "without" radiation case, as Rayleigh number increases enhancement in total Nusselt number continues**.**

The variation of the maximum temperature for each heater with Rayleigh number is shown in Fig. (7), for $A_R=5$, $N_R=1.5$, and $\varepsilon_h=\varepsilon_c=\varepsilon_a=0.5$. From the figure, it can be noticed that, as Rayleigh number increases, the maximum temperature decreases and the first heater (on the top) has the greatest temperature in the enclosure. The effect of the enclosure aspect ratio on the average Nusselt number is illustrated for each heater at $Ra=10^6$, $N_R=1.5$,

and $\varepsilon_h=\varepsilon_c=\varepsilon_a=0.5$ in Fig. (8a-d). The figure shows that the effect of the aspect ratio on the radiation mode heat transfer is insignificant. Furthermore, it is noticed that large increase of convective Nusselt number with the increase of the enclosure aspect ratio. Compared with "without" radiation case, a slight increase of the total Nusselt number with the increase of the enclosure aspect ratio is noticed. The effect of aspect ratio on the maximum heater temperature is depicted in Fig. (9). As the aspect ratio increases, the maximum temperature decreases. Also, surface radiation heat transfer leads to the decrease of the maximum temperature on the surface of the heaters for all aspect ratios considered in the present study, see Fig. (9).

The effect of surface radiation, represented by the radiation parameter N_R, on the average Nusselt number for the four discrete heaters is illustrated in Fig. (10a-d). From the figure it is can be concluded that the radiation Nusselt number increases as the radiation parameter increases, while the convection Nusselt number decreases as the radiation parameter increases. Furthermore, the figure shows increase of the total Nusselt number with the increase of the radiation parameter. Comparing with "without" radiation case, the surface radiation presented in radiation parameter, enhances the process of heat transfer.
Figure (11) shows the variation of the maximum dimensionless temperature on the heaters surfaces with the radiation parameter. It is noticed from the figure, that the maximum heaters surfaces temperature decreases markedly with the increase of the radiation parameter and this is due to heat transfer enhancement.

The effect of surface radiation on the heat transfer process is investigated by studying the effect of emissivity of the heaters surfaces on the average Nusselt number for each heater in Fig.(12a-d) for $Ra=10^6$, $N_R=1.5$, $\varepsilon_h=\varepsilon_c=\varepsilon_a=0.5$. It can be seen from the figure that as the emissivity of the heaters surfaces increases the radiation Nusselt number increases as well. Whereas the convection Nusselt number decreases and the total Nusselt number increases compared with the case of "without" surface radiation condition. The effect of heater emissivity, ε_h, on the maximum temperature of heaters is depicted in Fig.(13). For heater emissivity up to 0.6 a slight decrease of surface temperature with the increase of heaters emissivity is noticed. When ε_h increases above 0.6, a sharp decrease of the maximum temperature occurs. Finally, the effect of emissivity of both adiabatic and cold surfaces ε_a, ε_c respectively on the radiative heat transfer is investigated. However, it is found that their effects are insignificant. For the sake of brevity, only the effect of adiabatic surface emissivity is illustrated in Table (2).

Table 2. Effect of Adiabatic Surface Emissivity on the Maximum Dimensionless Temperature and Average Total Nusselt Number for AR= 5 , $\varepsilon_h = \varepsilon_c=0.5$, $N_R=1.5$ and Ra =10^6

ε_a	θ_{max}	Nu_h
0.2	0.13862	9.4677
0.3	0.13861	9.4654
0.4	0.13860	9.4657
0.5	0.13860	9.4695
0.6	0.13859	9.4660
0.7	0.13866	9.4665
0.8	0.13859	9.4666
0.9	0.13858	9.4672

The local temperature distribution on the left side (flush heater side) with and without radiation cases for different Rayleigh numbers is illustrated in Fig. (14). From the figure, it is depicted that the maximum temperature attained inside the enclosure is in the upper heater surface. Furthermore, the surface radiation decreases the temperature level due to the heat transfer enhancement especially at higher Rayleigh numbers.

5.3 Nusselt Number and Maximum Temperature Correlations

Based upon present numerical results, general correlations that accounts for the governing parameters were developed by expressing the average Nusselt number, its radiative and convective components on the heaters' surfaces as well as the maximum temperature that attained inside the enclosure as:

$$\overline{Nu} = 0.1796\, AR^{0.5563} Ra^{0.2387} \varepsilon_h^{0.1454} N_R^{\,0.1538} \tag{17a}$$

$$Nu_R = 5.339x10^{-5}\, AR^{0.3507} Ra^{0.0739} \varepsilon_h^{1.868} N_R^{\,2.0333} \tag{17b}$$

$$Nu_C = 0.3268\, AR^{0.5725} Ra^{0.1603} \varepsilon_h^{-0.1858} N_R^{\,-0.1782} \tag{17c}$$

$$\theta_{\max} = 4.823\, AR^{-0.497} Ra^{-0.214} \varepsilon_h^{-0.1655} N_R^{\,-0.1668} \tag{18}$$

with errors less than 9.5%

From the indices of the above correlation, it is clear that the relative powers reflect the influence of each parameter on the interaction between surface radiation and natural convection. While in the case of “without” surface radiation, the average Nusselt number and the maximum temperature inside the enclosure are given by:

$$\overline{Nu} = 0.284\, AR^{0.5944} Ra^{0.1848} \tag{19}$$

with an error of 9.5%

$$\theta_{\max} = 2.3596\, AR^{-0.5152} Ra^{-0.1057} \tag{20}$$

with an error of 0.1%

6. CONCLUSIONS

The interaction of surface radiation with natural convection in an air filled enclosures was investigated numerically. From the findings in the previous item of this paper, the following conclusions are drawn:

1. The increase of Rayleigh number leads to an increase of radiation Nusselt number while it leads to an increase of the convection Nusselt number to some value then decrease in convection Nusslet number with further increase of Rayleigh number.
2. Surface radiation enhances the heat transfer process as the total average Nusselt number taking into account surface radiation is higher than that of no radiation case.
3. The increase of Rayleigh number results in a decrease of maximum temperature than attained inside the enclosure.
4. The increase of enclosure aspect ratio has insignificant effect on the radiation Nusselt number whereas the increase of the enclosure aspect ratio increases the convection Nusselt number.
5. The maximum temperature that attained inside the enclosure decreases as the enclosure aspect ratio increases.
6. The emissivity of both cold and adiabatic surfaces has insignificant effect on the radiation Nusselt number.
7. The radiation Nusselt number increases with the increase of the emissivity of the heaters' surfaces whereas the convective Nusselt number decreases with the increase of heater surface emissivity.
8. The increase of radiation parameter leads to an increase of the radiation Nusselt number, a decrease in the convection Nusselt number and an increase of the total Nusselt number.
9. The increase of the radiation parameter leads to a considerable decrease of the maximum temperature that is attained in the enclosure.
10. Useful correlations are obtained for the average Nusselt number, its radiative and convective components as well as the maximum temperature that is attained inside the enclosure in terms of the parameters that govern the phenomenon of surface radiation interaction with the natural convection.

REFERENCES

1- Jaluria,Y.; “Natural Convection Cooling of Electronic Equipment, In Natural Convection: Fundamentals and Applications (Edited by S. Kack et al.) pp. 961-986. Hemisphere, Washington, D.C. 1985.
2- Incropera, F. P.; “Convection Heat Transfer in Electronic Equipment Cooling, ASME J. Heat Transfer 110. pp. 1097-1111, 1988.
3- Chu, H.H.S.; Churchill, S.W.; Patterson, C.V.S.; “The effect of Heater’s Size, Location, Aspect Ration and Boundary Condition in Two-dimensional Laminar Natural Convection in Rectangular Enclosure”, J. Heat Transfer 98, pp. 194-201, 1976.
4- Chadwick, M.I.; Webb, B.W.; Heaton, H.S.; “Natural Convection from two dimensional Heat Sources in a Rectangular Enclosure”, Int. J. Heat Mass Transfer 34, pp. 1679-1693, 1991.
5- Refai Ahmed, G.; Yovanovich, M.M.; “Influence of Discrete Heat Source Location on Natutral Convection Heat Transfer in a Vertical Square Enclosure”, J. Electronic Packaging, 113, pp. 268-274, 1991.
6- Ho, C.J.; Chang, J. Y.; “A Study of Natural Convection Heat Transfer in a Vertical Rectangular Enclosure with Two-dimensional discrete Heating Effects of Aspect Ratio”, Int. J. Heat Mass Transfer 37, 917-925, 1994.
7- Hoogendoorn, C.J. “Experimental Methods in Natural Convection, Fundamentals and Applications”, Kakac, S.; Awang, W. and Viskanta, R. (eds.), 1985.

8- Larson, D.W.; Viskanta, R. “Transient Combined Laminar Free Convection and Radiation in a Rectangular Enclosure,” J. Fluid Mech. 78, pp. 65-85, 1976.
9- Kim, D.M.; Viskanta, R. “Heat Transfer by Conduction, Natural Convection and Radiation across a Rectangular Cell Structure”, Int. J. Heat Fluid Flow 5, pp. 205-213, 1984.
10- Balaji, C.; Venkateshan, S.P., “Interaction of Surface Radiation with Free Convection in Square Cavity”, Int. J. of Heat and Fluid Flow, Vol. 14, No. 3, Sept. 1993.
11- Asako, Y.; Nakamura, H. “Heat Transfer across a Parallogram Shaped Enclosure”, Bull. JSME 25, pp.1412-1424, 1982.
12- Ho, C.F.; Chang, J.Y. “Effect of Surface Radiation on Natural Convection-air Cooling of Discrete Heaters in Vertical Enclosures”, J. Heat Transfer 30, pp. 27-32, Spriger-Verlag, 1994.
13- Hottle, H.C.; Sarafim, A.S., Radiative Heat Transfer; Mc-Graw Hill, New York, 1967.
14- Ho, C.J.; Chang, J.Y., "Study of Natural Convection Heat Transfer in a Vertical Rectangular Enclosure with Two-Dimensional Discrete Heating: Effect of Aspect Ratio", Int. J. Heat Mass Transfer, Vol. 37, No. 6, pp. 917-925, 1994
15- Rao, S.S., The Finite Element Method in Engineering, Pergamon press, 1982.
16- Pepper, D.W.; Heinrich, J.C., The Finite Element Method – Basic Concepts and Applications, Hemisphere Pub. Corporation, 1992.
17- Ramesh, N. ; Venkateshan, S.P., "Effect of Surface Radiation and Partition Resistance on Natural Convection Heat Transfer in Partitioned Enclosure: An Experimental Study", Trans. of ASME, Vol. 121, Aug. 1999.

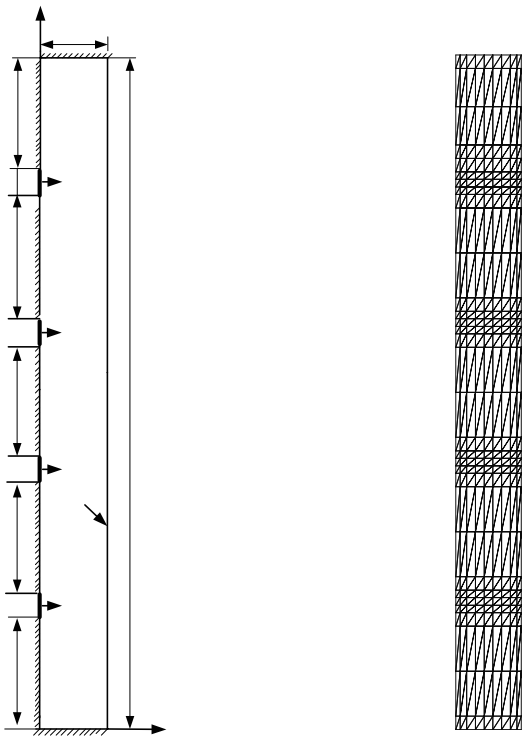

(a) (b)

Fig.1. (a) Schematic diagram of the physical domain and coordinate system
(b) Finite element discritization for the solution domain.

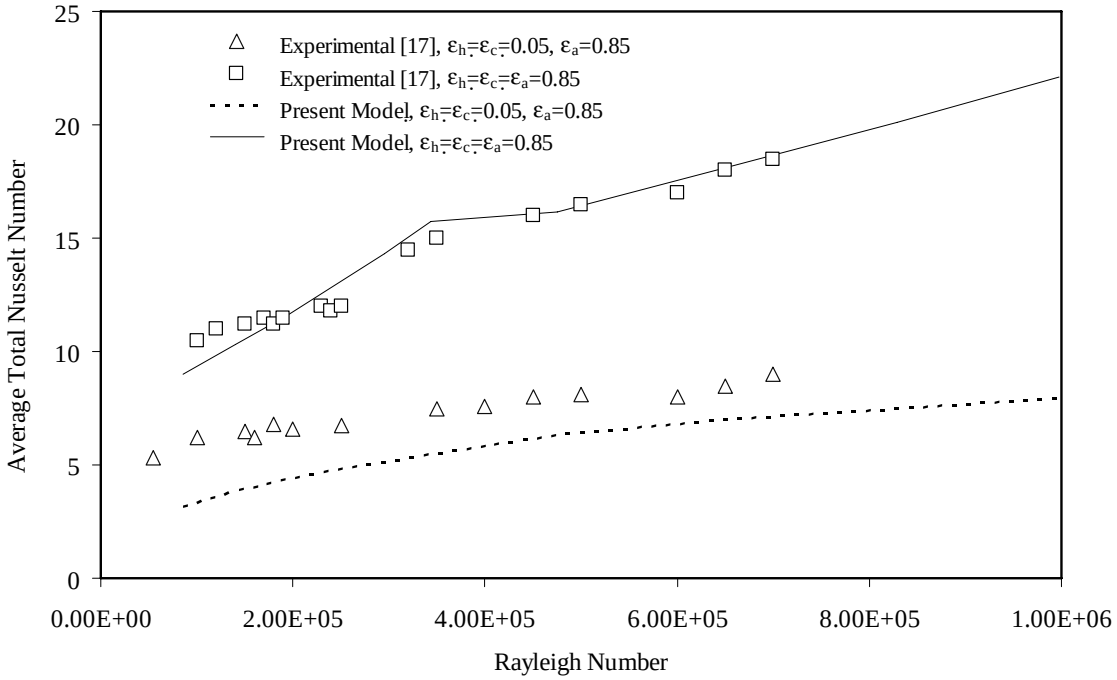

Fig. 2. Comparison between the present model prediction and the experimental data [17].

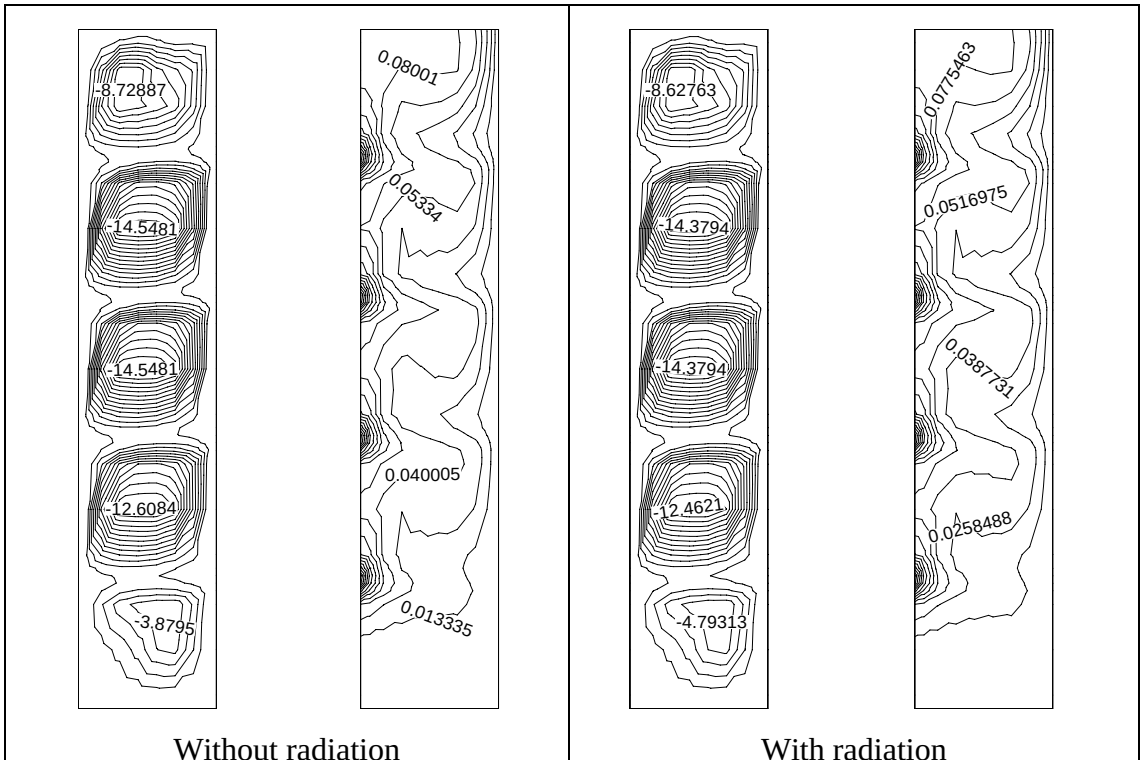

Fig. 3. Effect of surface radiation on the structures of streamlines (left) and isotherms (right), $Ra=10^5$, $N_R=1.5$, AR=5, $\varepsilon_h=\varepsilon_c=\varepsilon_a=0.5$

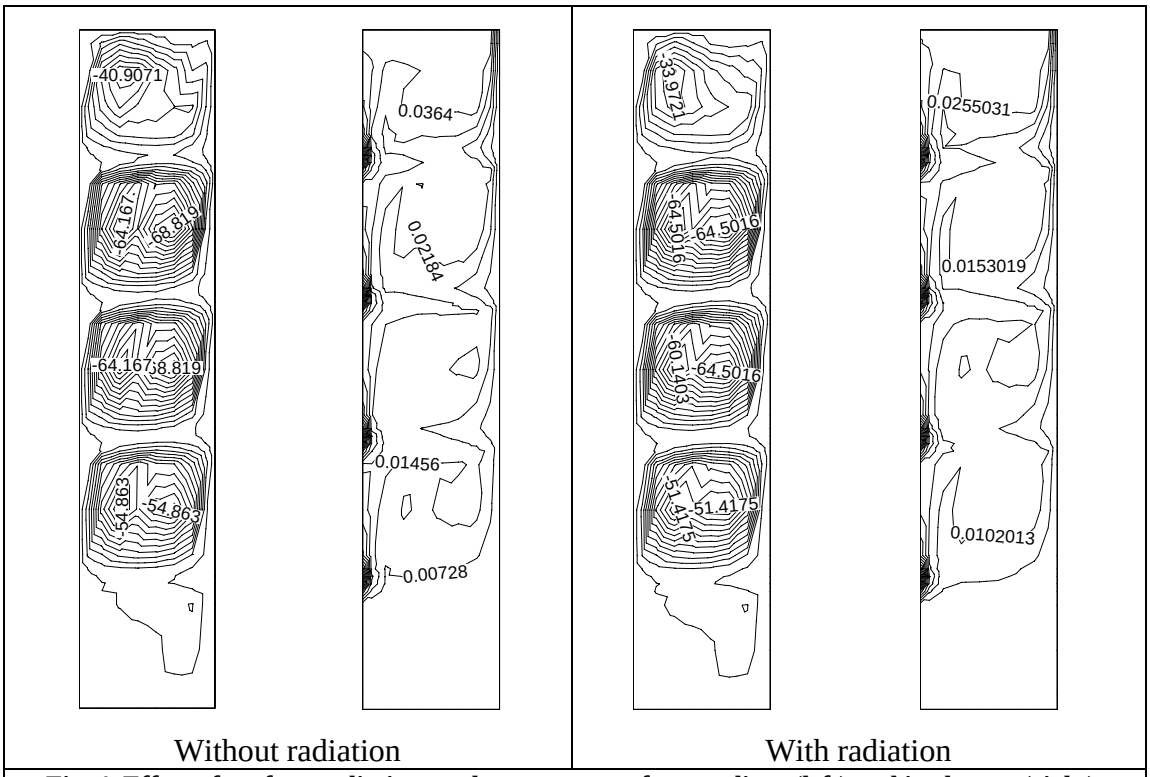

Fig. 4. Effect of surface radiation on the structures of streamlines (left) and isotherms (right), $Ra=5x10^6$, $N_R=1.5$, AR=5, $\varepsilon_h= \varepsilon_c=\varepsilon_a=0.5$.

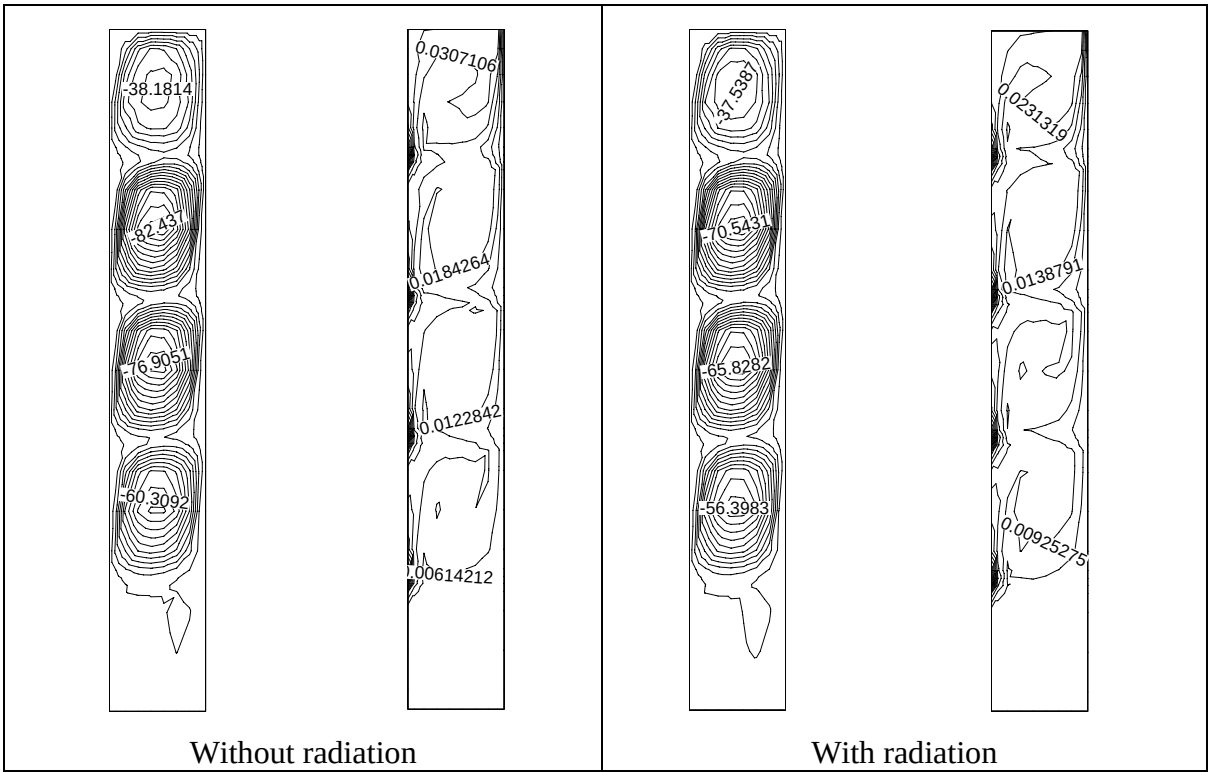

Fig. 5. Effect of surface radiation on the structures of streamlines (left) and isotherms (right), $Ra=5x10^6$, $N_R=1.5$, AR=7, $\varepsilon_h= \varepsilon_c=\varepsilon_a=0.5$.

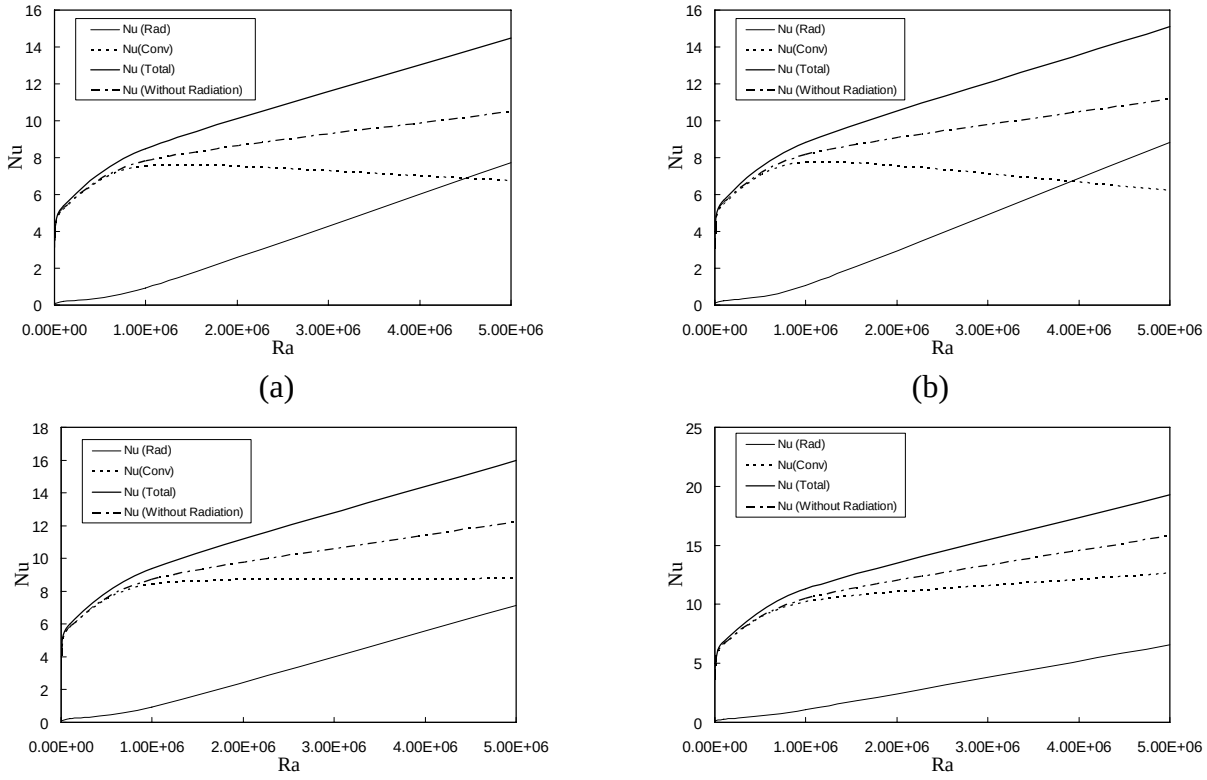

Fig.6. The variation of the average Nusselt number with Rayleigh number for (AR=5, N_R=1.5, $\varepsilon_h=\varepsilon_c=\varepsilon_a$=0.5) (a) First heater (b) Second heater (c) Third heater (d) Fourth heater.

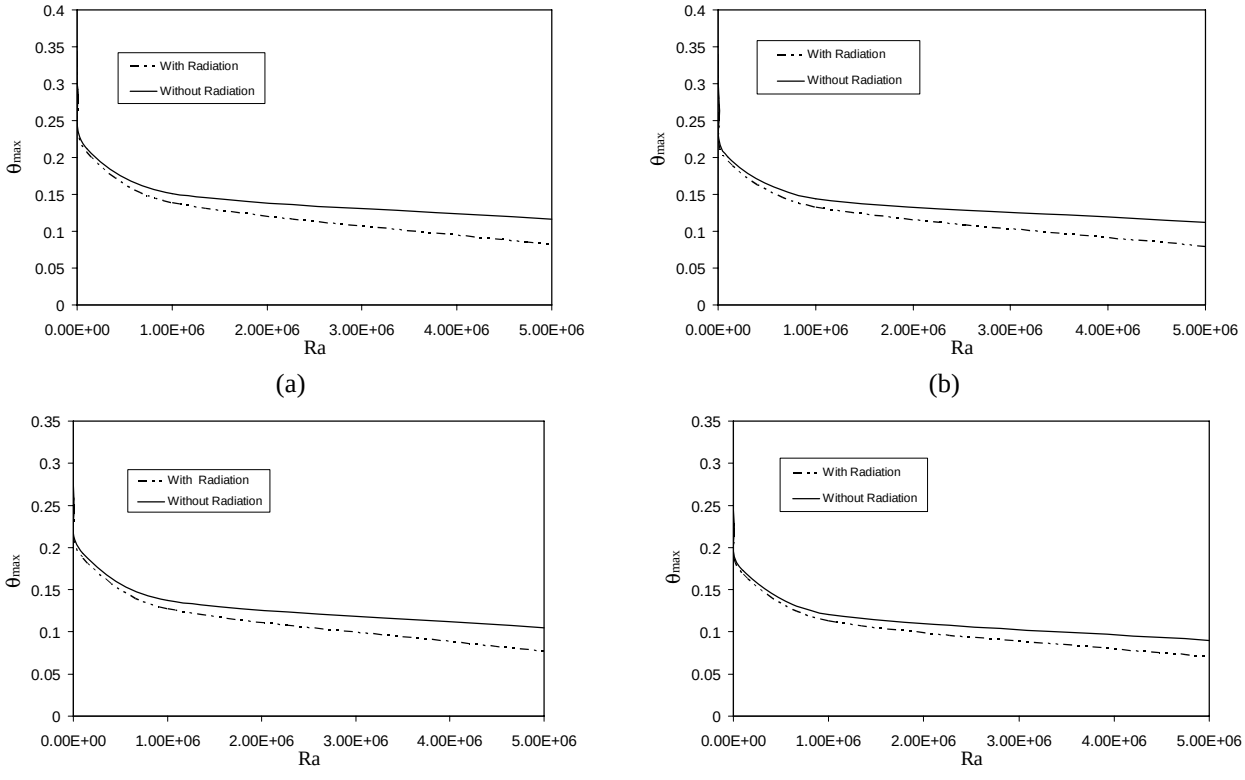

Fig.7. The variation of the maximum dimensionless temperature with Rayleigh number for (AR=5, N_R=1.5, $\varepsilon_h=\varepsilon_c=\varepsilon_a$=0.5) (a) First heater (b) Second heater (c) Third heater (d) Fourth heater

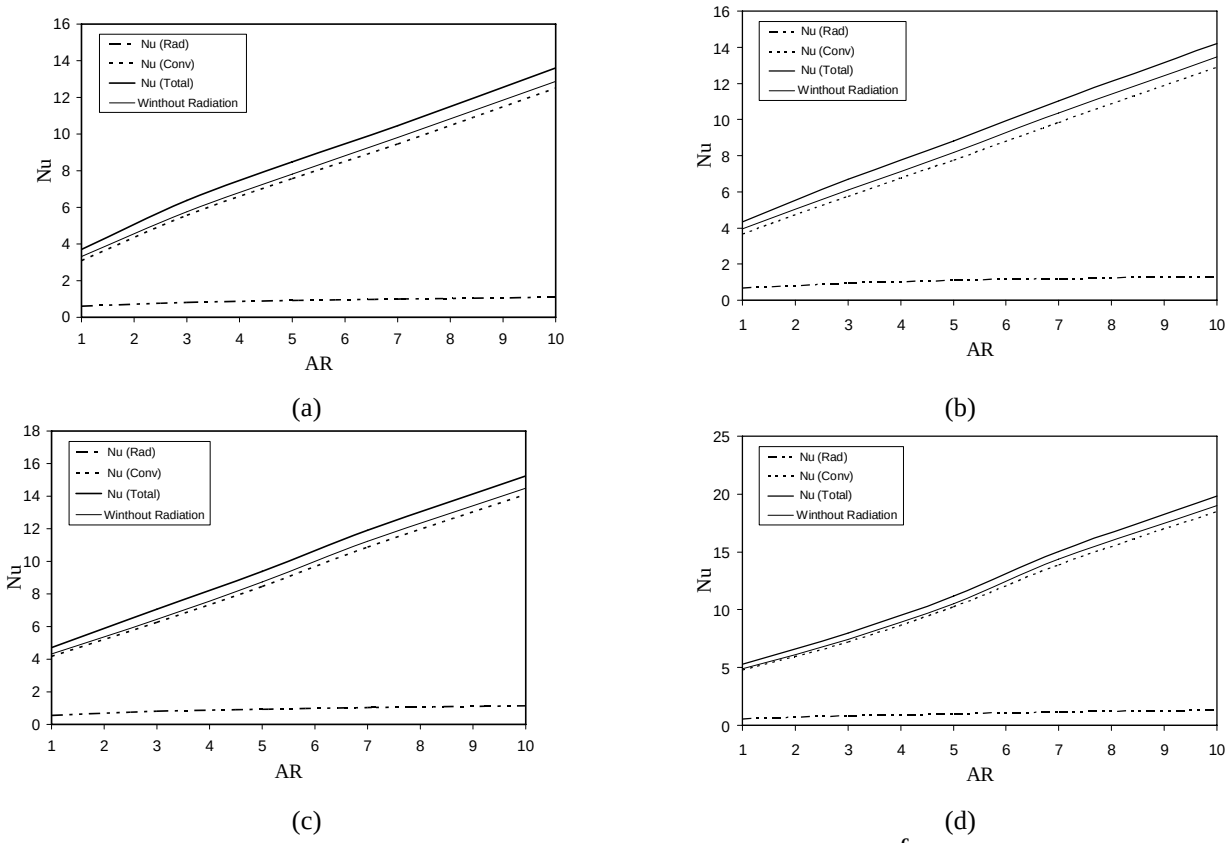

Fig.8. The variation of the average Nusselt number with aspect ratio for ($Ra=10^6$, $N_R=1.5$, $\varepsilon_h=\varepsilon_c=\varepsilon_a=0.5$) (a) First heater (b) Second heater (c) Third heater (d) Fourth heater

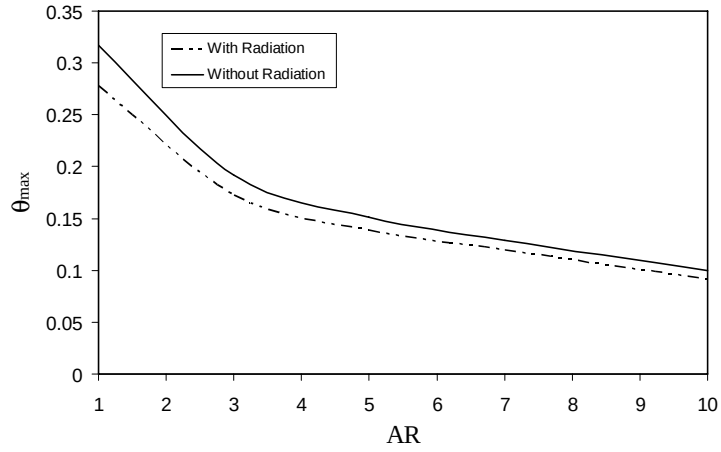

Fig.9. The variation of the maximum dimensionless temperature with aspect ratio for ($Ra=10^6$, $N_R=1.5$, $\varepsilon_h=\varepsilon_c=\varepsilon_a=0.5$).

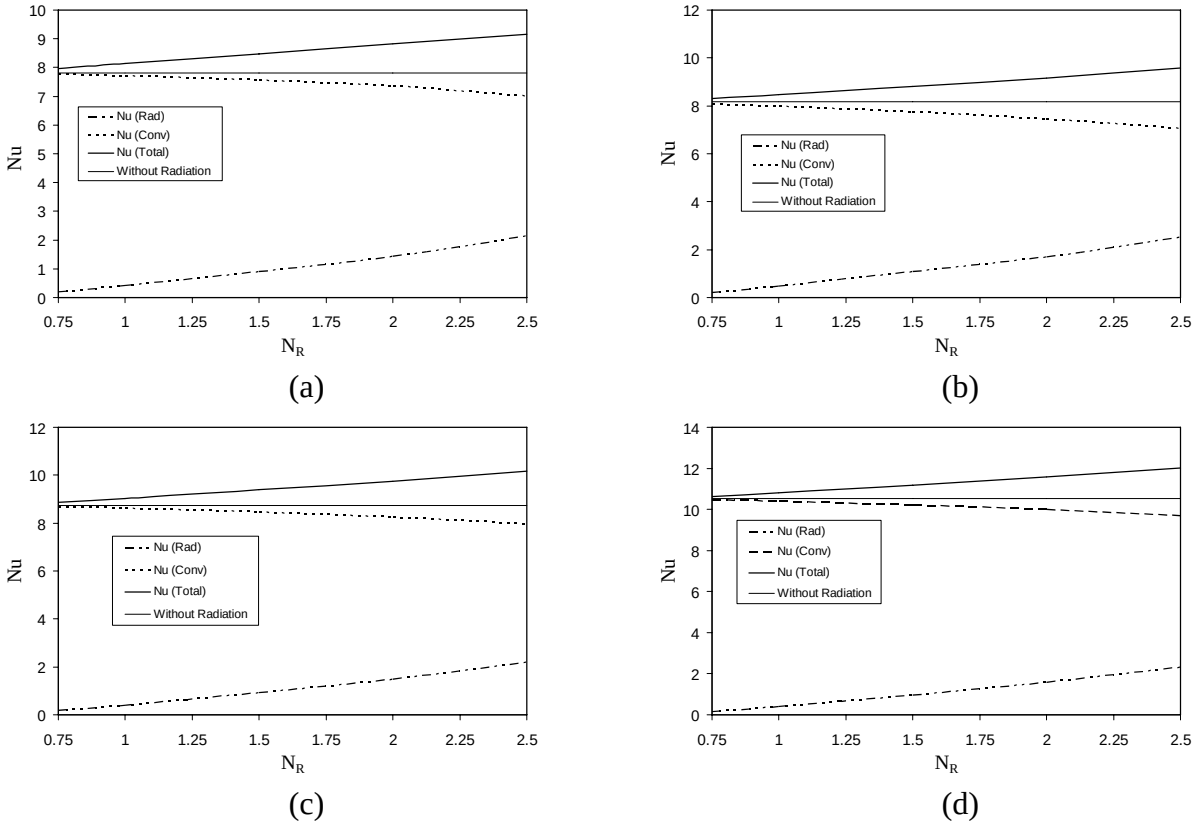

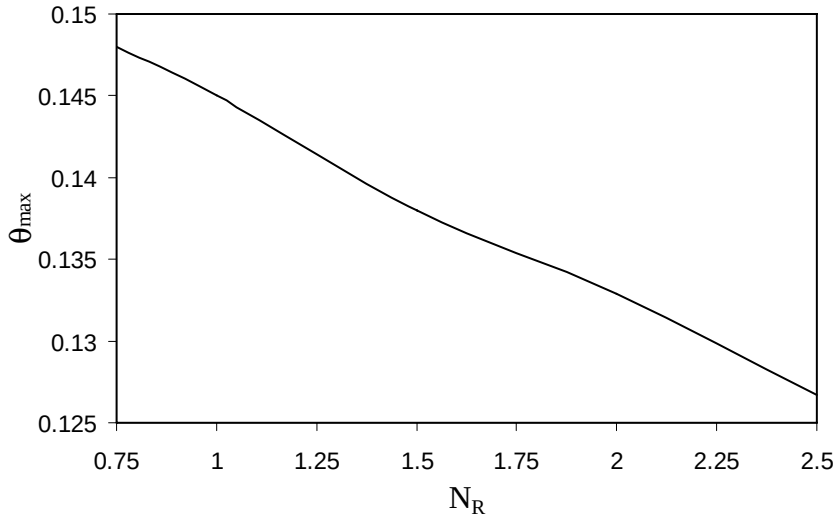

Fig. 11. The variation of the maximum dimensionless temperature with the radiation parameter for ($Ra=10^6$, AR=5, $\varepsilon_h=\varepsilon_c=\varepsilon_a=0.5$).

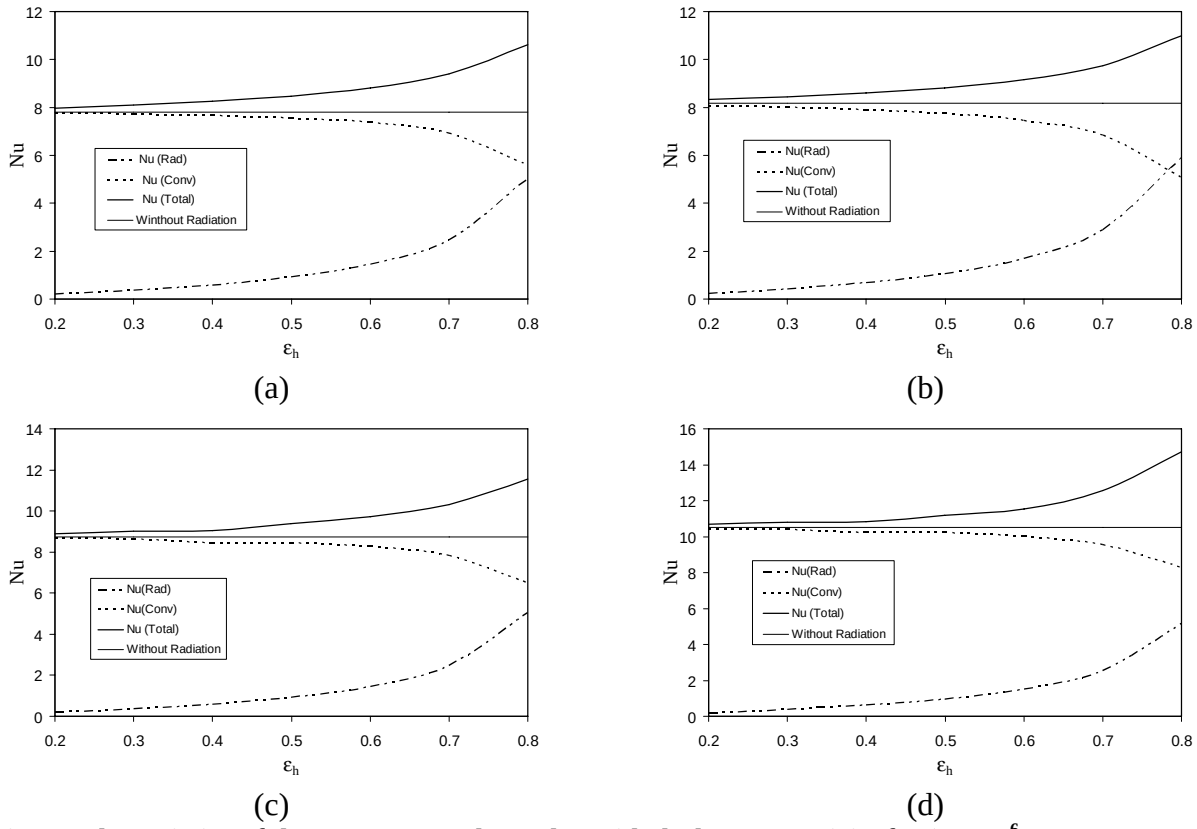

Fig. 12. The variation of the average Nusselt number with the heater emssivity for ($Ra=10^6$, AR=5, N_R=1.5, $\varepsilon_c=\varepsilon_a$=0.5) (a) First heater (b) Second heater (c) Third heater (d) Fourth heater

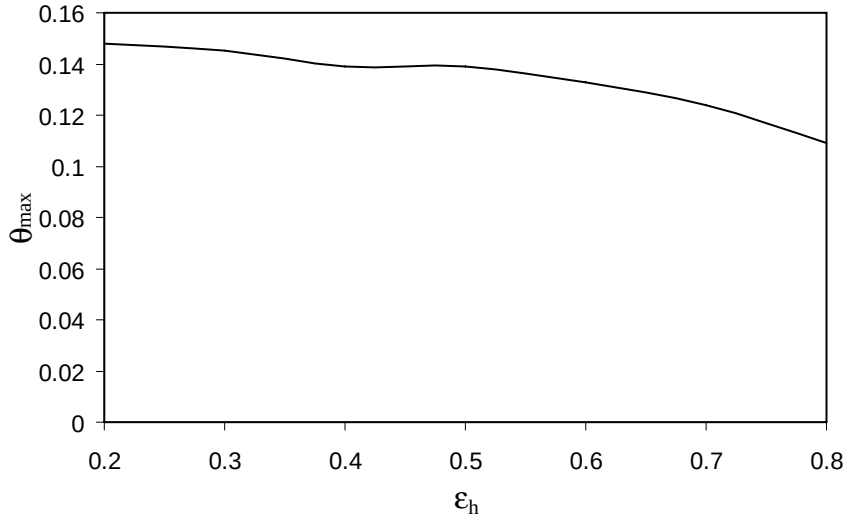

Fig. 13. The variation of the maximum dimensionless temperature with the heater emissivity for ($Ra=10^6$, AR=5, $N_R=1.5$, $\varepsilon_c=\varepsilon_a=0.5$).

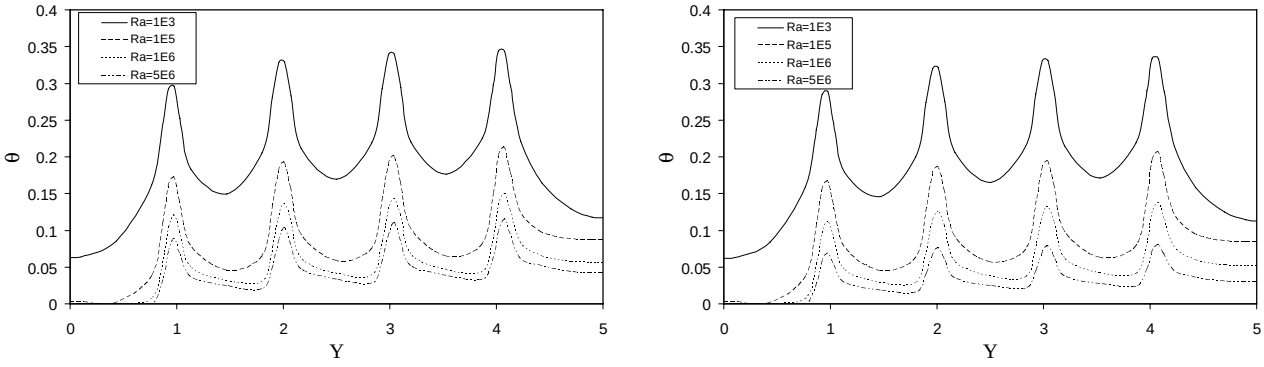

Without radiation With radiation

Fig.14. The variation of the maximum dimensionless temperature with aspect ratio.